Force-dependent binding of vinculin to α-catenin regulates cell-cell contacts stability and collective cell behavior

Rima Seddiki[1], Pierre-Olivier Strale[1,2], Grégoire Peyret[1], Mingxi Yao[2], Jie Yan[2], Benoit Ladoux[1,2] and René Marc Mège[1,*]

[1] Institut Jacques Monod, CNRS, Université Paris-Diderot, 15 Rue Hélène Brion 75205 Paris Cedex 13, France

[2] Mechanobiology Institute, National University of Singapore, 5A Engineering Drive 1, Singapore 117411, Singapore

*Corresponding author: René Marc Mège, Institut Jacques Monod, 15 Rue Hélène Brion, 75205 Paris Cedex, France, tel : 33 1 57 2780 67, mail : rene-marc.mege@ijm.fr

Running title: α-catenin/vinculin AJ mechanosensor

Summary statement: Combining cell biology and biomechanical analysis, we show here that the coupling between cadherin complexes and actin trough tension-dependent α-catenin/vinculin association is regulating AJ stability and dynamics as well as tissue-scale mechanics.

Keywords: adherens junction, α-catenin, mechanotransduction, actomyosin, collective cell migration, E-cadherin

Abstract

The shaping of a multicellular body and repair of adult tissues require fine-tuning of cell adhesion, cell mechanics and intercellular transmission of mechanical load. *Adherens* junctions (AJs) are the major intercellular junctions by which cells sense and exert mechanical force on each other. However, how AJs adapt to mechanical stress and how this adaptation contributes to cell-cell cohesion and eventually to tissue-scale dynamics and mechanics remains largely unknown. Here, by analyzing the tension-dependent recruitment of vinculin, α-catenin and F-actin in function of stiffness, as well as the dynamics of GFP-tagged wt and mutated α-catenins, altered for their binding capability to vinculin, we demonstrate that the force-dependent binding of vinculin stabilizes α-catenin and is responsible for AJ adaptation to force. Challenging cadherin complexes mechanical coupling with magnetic tweezers, and cell-cell cohesion during collective cell movements, further highlight that tension-dependent adaptation of AJs regulates cell-cell contact dynamics and coordinated collective cell migration. Altogether, these data demonstrate that the force-dependent α-catenin/vinculin interaction, manipulated here by mutagenesis and mechanical control, is a core regulator of AJ mechanics and long-range cell-cell interactions.

Introduction

Adherens junctions (AJs) contribute both to tissue stability and dynamic cell movements. The cadherin-catenin adhesion complex is the key component of AJ that bridges neighboring cells and the actin-myosin cytoskeleton, and thereby contributes to mechanical coupling between cells which drives both cell assembly stability and dynamic cell movements during morphogenetic and tissue repair events (Collins and Nelson, 2015; Guillot and Lecuit, 2013; Mayor and Etienne-Manneville, 2016; Takeichi, 2014). Central to this process is the dynamic link of the complex to actin filaments (F-actin) (Mege and Ishiyama, 2017). Cadherin cytoplasmic tail binds to β-catenin, which in turn binds to the F-actin binding protein α-catenin. α-catenin then links cadherin-β-catenin adhesion complexes to the force-generating actomyosin networks, directly and/or indirectly through other actin binding proteins such as vinculin or afadin.

In addition, mechanotransduction at AJs enables cells to sense, signal, and respond to physical changes in their environment, and the cadherin-catenin complex has emerged as the main route of propagation and sensing of forces within epithelial and non-epithelial tissues (Hoffman and Yap, 2015; Huveneers and de Rooij, 2013; Ladoux et al., 2015; Leckband and Prakasam, 2006). A proposed mechanotransduction pathway involves the myosin II-generated force-dependent change of conformation of α-catenin regulating vinculin recruitment (le Duc et al., 2010; Thomas et al., 2013; Yonemura et al., 2010). At the single molecule level, it has been shown that α-catenin reversible unfolds upon forces in the range of those developed by a few myosin motors, allowing the binding of vinculin head (Maki et al., 2016; Yao et al., 2014). The tension-dependent binding of vinculin to α-catenin may thus be central for the adaptation of cadherin-

dependent cell-cell contacts experiencing tugging forces in dynamic epithelial layers (Han et al., 2016; Jurado et al., 2016; Kim et al., 2015), and may contribute directly to tissue mechanics and collective cell behavior. However, how this molecular pathway contributes to the dynamics of cell-cell contacts, and allow cells to locally sense, transduce and adapt to environmental mechanical constraint, is not well understood.

Here, we tested this hypothesis by investigating the contribution of the interaction between vinculin and α-catenin to AJ dynamics and collective cellular behavior. Indeed, it has been difficult to address this question so-far, at least in mammalian cells, since in addition of the pleiotropic effect of α-catenin loss of function described *in vivo* (Lien et al., 2006; Silvis et al., 2011; Torres et al., 1997; Vasioukhin et al., 2001), the knock-out of the protein in cells *in vitro* lead to the complete inhibition of cadherin-mediated adhesion (Benjamin et al., 2010; Thomas et al., 2013; Vermeulen et al., 1995), as well as to cadherin-independent alteration of actin dynamics affecting cell interaction with the ECM (Benjamin et al., 2010; Hansen et al., 2013). To address directly the role of the tension-dependent association of α-catenin and vinculin, we generated mutant α-catenin proteins either unable to bind vinculin or constitutively bound to vinculin, and analyzed their effect on cell-cell contact stability and collective cell behavior when expressed in α-catenin-depleted epithelial cells.

Results and discussion

α-Catenin, vinculin and F-actin recruitment at cell-cell contacts is dependent on intercellular tension in epithelial monolayers

Previous data have shown that vinculin recruitment at cell-cell contacts was dependent on both internal cell contractility (le Duc et al., 2010; Yonemura et al., 2010) and externally applied forces (Dufour et al., 2013; le Duc et al., 2010). However, these data were obtained either by inhibiting intracellular contractility or by applying external forces. Here, to determine the impact of intercellular stress physiologically generated by cell-born contractile forces on AJs, we plated MDCK cells on fibronectin (FN)-patterned polyacrymamide (PAA) gels of controlled stiffness's ranging from 4.5, 9 and 35 kPa and looked at the impact of stiffness on the recruitment of αE-catenin (referred to as α-catenin), vinculin and F-actin. The junctional recruitment of α-catenin, vinculin and F-actin significantly increased with substrate stiffness **(Fig. 1A,B)**. This enrichment did not result from increased cellular levels in proteins as shown by western blot **(Fig. 1C)**. Thus, the junctional recruitments of α-catenin, vinculin and F-actin are positively controlled by the intercellular tension imposed by the matrix stiffness. The staining at cell-cell contacts with an antibody recognizing α-catenin under its open conformation also significantly increased with substratum rigidity, suggesting a central contribution of the tension-dependent conformational change of α-catenin and recruitment of vinculin to the physiological adaptation to force of AJs.

Vinculin binding to α-catenin is not required for the formation of cell-cell junctions but *stabilizes junctional α-catenin*

To address the role of the α-catenin/vinculin interaction in the tension-dependent regulation of cell-cell contacts, we generated α-catenin mutants unable to bind vinculin (α-cat-L344P-GFP) or binding constitutively to vinculin (α-cat-Δmod-GFP) **(Fig. 2A)**. Vinculin binds to α-catenin within the MI domain, and substitution of Lysine 344 by Proline was reported to impair vinculin binding (Peng et al., 2012; Yao et al., 2014). The MII and MIII domains (residues 509-628) are auto-inhibitory domains interacting with the M1 domain and masking the accessibility of the vinculin binding domain (Desai et al., 2013; Maki et al., 2016). This auto-inhibition is released upon force-dependent stretching of the molecule, unmasking the vinculin binding domain (Yao et al., 2014). Deletion of residues 509-628 (Δmod mutation) thus generates a α-catenin isoform constitutively binding to vinculin.

We analyzed the consequences of the expression of these two variants on cell-cell contact restoration in α-catenin-depleted MDCK cells, that do not form AJs (Benjamin et al., 2010). The expression of α-cat-L344P-GFP and α-cat-Δmod-GFP restored the formation of cell-cell contacts that were indistinguishable from those of wt α-catenin expressing cells (α-cat-wt-GFP) **(Fig. 2B)**. The recruitment of vinculin at intercellular junctions was significantly higher in α-cat-Δmod-GFP than in wt-α-cat-GFP expressing cells (1.04 ± 0.02, n= 20 versus 0.67 ± 0.01, n =31, p value < 0.0001) and reduced in α-cat-L344P expressing cells (0.34 ± 0.06, n=24) compared to wt-α-cat expressing cells (p value < 0.0001), while the recruitment of vinculin at the cell-substratum interface was comparable for the three cell types **(Fig. S1)**. Thus, the two forms of α-catenin allow the formation of AJs in confluent MDCK monolayers, despite their impaired interaction with vinculin. The residual accumulation of vinculin at cell-cell contacts in α-cat-Δmod-GFP

cells may result from the interaction of vinculin with β-catenin reported previously (Peng et al., 2010; Ray et al., 2013). To assess the effect of vinculin-α-catenin interaction on the stability of AJs, we performed FRAP experiments on GFP-α-catenins at cell-cell contacts. The fluorescence recovery was similar for wt and Δmod α-catenin with ~ 50 % the molecules in the fast recovering, diffusion-limited fraction **(Fig. 2C, D)**. However, the fluorescence recovery for the L344P mutant was significantly increased with a mobile fraction of α-catenin that was doubled **(Fig. 2C, D)** without changes in half recovery time **(Fig S2A).** Interestingly, E-cadherin stability at cell-cell contacts was barely dependent on the binding of α-catenin to vinculin **(Fig. S3A, B)**. Thus, vinculin binding to α-catenin is dispensable for the formation of intercellular contacts *per se*, but is required for the stabilization of junctional α-catenin in confluent monolayers. Vinculin may stabilize α-catenin at AJs by providing additional binding interfaces between cadherin/α-catenin complexes and F-actin, thanks to its F-actin binding domain (Thomas et al., 2013; Yonemura et al., 2010). Previous studies indicate that the anchoring of cadherin/catenin complexes to F-actin by the actin binding site of vinculin in the absence of α-catenin actin binding domain is sufficient to restore E-cadherin dependent cell contacts (Chen et al., 2015; Jurado et al., 2016; Thomas et al., 2013) and that these junctions are even more stable than wt AJs (Chen et al., 2015). Vinculin incorporation in the adhesion complexes may thus increase their stability. Furthermore, since vinculin binding is under the control of tension-dependent conformational switch of α-catenin, these protein-protein interactions may be favored upon increased myosin-II generated cell contractility and explain the observed substrate rigidity-dependent recruitment of AJ components.

Binding of vinculin is required for the tension-dependent stabilization of α-catenin at cell-cell contacts

To further determine the requirement of the α-catenin/vinculin interaction in the tension-dependent adaptation of cell-cell contacts, we analyzed the dynamics of junctional α-cat-wt, α-cat-L344P and α-cat-Δmod in cells seeded on PAA substrates of 4.5 or 35 kPa stiffness's **(Fig. 3)**. FRAP experiments performed on α-cat-WT expressing cells revealed a significant stiffness-dependent change in junctional α-catenin dynamics, with a higher mobile fraction on the more compliant substrate **(Fig. 3A, C)**. At the opposite, the dynamic of the α-catenin mutants were independent of substrate stiffness **(Fig. 3B, C)**. The mobile fraction α-cat-L344P-GFP was similar on both substrates and comparable to the mobile fraction value observed for the wt α-catenin on soft substrate. The mobile fraction of junctional α-cat-Δmod-GFP was also independent of the substratum compliance, but was significantly lower and comparable to the value obtained for wt α-catenin on stiff substrate. The characteristic recovery half times were not significantly different among these different conditions **(Fig S2B)**. The dynamics of E-cadherin did not change significantly with substrate compliance, or with α-catenin mutations **(Fig. S3)**, in agreement with the observed vinculin-independent recruitment of E-cadherin around cell-bound E-cadherin-coated beads (le Duc et al., 2010). These data show that the molecular stability of α-catenin at AJs is mechanosensitive, and that this mechanosensitive stabilization requires the binding to vinculin. Altogether, they suggest that the tension-dependent binding of vinculin to α-catenin regulates the stiffness-dependent stabilization of cadherin adhesion complexes at cell-cell contacts.

Vinculin/α-catenin association controls E-cadherin coupling to cortical actin

We proposed that vinculin binding may control cell-cell mechanical coupling by affecting the association of cadherin complexes to the underlying actin cytoskeleton. To test this hypothesis, we performed magneto-cytometry experiments using super-paramagnetic Ecad-Fc-coated bead doublets bound on α-cat-wt, α-cat-L344P, α-cat-Δmod expressing cells. The bead doublets were made by mixing antibody immobilized Ecad-Fc-coated beads with Protein A coated beads therefore only one bead of the doublet binds to the cell through E-cadherin interaction. Torque were applied to bound bead doublets by rotating a pair of permanent magnets 360 degrees in both clockwise and counter clockwise direction, and the fluctuation angles of the bead doublets were analyzed to obtain their response to the applied torque **(Fig. 3D**). This measurement can be considered as a proxy of the stiffness of the mechanical link between cadherins and the cell cortex (le Duc et al., 2010). Surprisingly, the bead fluctuation angles showed two populations for cells expressing α-cat-wt, with half the beads loosely attached (mean standard deviation = 51.8 ± 3.8 °) and the other half strongly coupled (mean s.d. = 9.2 ± 2.9 °), indicating a complex regulation of the linkage between cadherin complexes and the cell cortex. The mean s.d. of the bead fluctuation angle was centered to 25.1 ± 7.5 degrees for cells expressing α-cat-L344P, indicating a very loose coupling to the cell cortex. At the opposite the mean s.d. was close to 0 (3.5 ± 1.8 °) for cells expressing α-cat-Δmod, indicating a very stiff link of cadherins to the cortical actin **(Fig. 3D)**. These results demonstrate that the binding of α-catenin to vinculin is required for efficient mechanical coupling of cadherin-catenin complexes to the cytoskeleton, a result reminiscent of the requirement of vinculin for the force-dependent stiffening of E-

cadherin junctions observed in F9 cells (le Duc et al., 2010). For reasons we do not understand yet, E-cadherin beads bound to wt α-catenin expressing cells were either tightly or loosely coupled to the cortical cytoskeleton as if the interaction was bi-stable. Whether the two states were associated to differences in the lifetime of the bead-cell contact or to specific sites of binding of the bead on the cell surface are questions that could not be addressed with the present approach. However, the results obtained with mutants show that α-catenin binding to vinculin is required for efficient mechanical coupling of cadherin to the cytoskeleton. Altogether, our findings open the possibility that the mechanosensitive α-catenin/vinculin interaction by contributing to tension-dependent cell-cell contacts stability regulates tissue mechanics.

Vinculin/α-catenin association controls collective cell dynamics

Previous studies have unraveled the essential role of α-catenin in maintaining tissue cohesion and collective cell behavior (Bazellieres et al., 2015; Doxzen et al., 2013; Vedula et al., 2012). However, the contribution of the tension-dependent association of vinculin to α-catenin in this process remains unknown. To address the specific role of the binding of vinculin to α-catenin, we studied the movement of confluent MDCK cells seeded on FN-coated circular patterns (**Fig. 4A**). The dynamics of mutant monolayers were analyzed and compared to those of α-cat-wt expressing and parental α-cat KD cells monolayers **(Suppl. Videos 1 to 4)**. α-cat-Δmod and α-cat-wt monolayers displayed slow and coordinated movements. At the opposite, α-cat KD and α-cat-L344P cells behave as mesenchymal-like cells, displayed more rapid and uncoordinated motions as described previously for α-cat KD cells (Vedula et al., 2012). The heat map of velocity fields

obtained by Particle Imaging Velocimetry (PIV, supplemental methods) analysis further revealed higher velocities for α-cat KD and α-cat-L344P cells than for α-cat-Δmod and α-cat-wt cells (**Fig. 4B)**. The average velocities were the highest for α-cat KD cells, then significantly decreased for α-cat-L344P cells, and finally for α-cat-wt and α-cat-Δmod cells (**Fig. 4C)**. The spatial velocity correlation which refers to the mean distance at which velocity vectors are oriented in the same direction length was further extracted as a quantitative parameter of cell movement coordination. α-cat KD cells exhibited low coordinated in motion with a correlation length of 50 μm as opposed to values around 150-200 μm for wt MDCK cells, as reported by (Vedula et al., 2012). Correlation lengths were comparable for α-cat-Δmod and α-cat-wt cells. However, the correlation length was significantly lower for α-cat-L344P than for α-cat-wt cells denoting an altered coordinated behavior (**Fig. 4D)**. Collective epithelial cell movements are thus strongly dependent on the ability of α-catenin to bind vinculin.

An increased stability of cell-cell contacts, by limiting neighbor exchange within the monolayer, may directly explain a more coordinated cell behavior and vice versa. This was confirmed by quantifying the effect of vinculin-binding capability of α-catenin on the lifetime of cell-cell contacts in monolayers coexpressing RFP-Ftractin (**Fig. 4E, Suppl. Videos 5 to 8)**. While cell-cell contact lifetime was of less than 1 hour for α-cat KD cells, it was of 4.7 ± 2.6 h for α-cat-L344P cells and increased to 7.7 ± 3.4 h and 12.6 ± 6.1 h for α-cat-wt and α-cat-Δmod cells, demonstrating that the binding of vinculin to α-catenin is required for maintaining stable cell-cell contacts during collective motion of epithelial cells. Thus, we show here that coordinated motion of epithelial cells is

dependent on the ability of α-catenin to bind vinculin, which drastically increase cell-cell contact lifetime.

Altogether our results show that the force-dependent interaction between α-catenin and vinculin is crucial for epithelial cells to develop stable but adaptive cell-cell contacts in response of the mechanical resistance of their environment as well as for long-range cell-cell interactions and tissue-scale mechanics. The fact that the association between the two proteins, manipulated here by mutagenesis and mechanical control, has a direct incidence on collective cell movements put the core α-catenin and vinculin mechanosensing machinery at the center of the control of morphogenetic processes.

Material and Methods

Cell culture

Madin-Darby canine kidney (MDCK, from ATCC) and MDCK αE-catenin knockdown cells (Benjamin et al., 2010) were maintained in DMEM/Glutamax 10% fetal bovine serum (FBS), 100 µg/mL penicillin/streptomycin at 37°C in 5% CO_2. Cells were electroporated using Amaxa system (Nucleofector Device, Lonza) under the following conditions 24 hours prior to experiments: 1.10^6 cells, kit L, 5 µg of DNA.

Expression vectors

The wt GFP-α-catenin expression vector coding for GFP fused in N-terminal of mouse αE-catenin was described previously (Thomas et al., 2013). L344P GFP-α-catenin was derived from the wt construct by PCR and DNA ligation. Δmod GFP-α-catenin was obtained by deleting the sequence coding for residues 509-628 (domains MII and MIII according to (Desai et al., 2013)).

Immunofluorescent staining

Cells were fixed for 15 min with PBS, 4% formaldehyde, permeabilized with 0.15% Triton X-100 in PBS for 5 min, then incubated with primary antibodies (anti-vinculin mouse monoclonal antibody (1/200, clone 7F9, Millipore), rabbit polyclonal anti-α-catenin and anti-β-catenin (1/400, Sigma), rat α18 monoclonal anti-αE-catenin antibody (1/200, A. Nagafuchi, Kumamoto Univ.) in PBS, 1.5% BSA for 2 hours at room temperature. The secondary antibodies (Jackson Laboratories) and Alexa-643 phalloidin (Molecular Probes) were incubated for 1 hour in PBS-BSA.

Micropatterning

PDMS (Poly-dimethylsiloxane) stamps were molded and cured as described previously (Vedula et al., 2014) on silicium wafers (IEMN (Lille, France) or MBI (NUS, Singapore)). A thin layer of PDMS was spin coated over a 35 mm plastic petri dish and cured at 80^{o}C for 2 hours, then exposed to UV for 15 min in a UVO cleaner (Jelight Company Inc.). PDMS stamps were incubated with a solution of FN/Cy3-conjugated FN (10/1 ratio, 50 µg/ml, Millipore) for 45 min, washed with water and air dried, then gently pressed against the surface to transfer FN. Regions outside the patterns were blocked with 0.2% Pluronics F-127 (Sigma) for 1 hour and washed 3 times with PBS.

Alternatively, polyacrylamide (PAA) substrates were patterned. For this, air dried FN-coated PDMS stamps were brought into contact with a cleaned 22 mm by 22 mm glass coverslip. A second cleaned coverslip, serving as the base for the gel, was silanized by dipping in ethanol solution containing 2% (v/v) 3-(trimethoxysilyl) propyl methacrylate silane (Sigma) and 1% (v/v) acetic acid for 5 min. 20 µl of PAA solution were placed between the silanized coverslip and the FN-stamped one. After 45min of polymerization the patterned coverslip was removed and the coverslip with the gel, on which patterned FN had been transfered, placed in a solution of 10 mM HEPES.

Videomicroscopy

Transfected cells were seeding at subconfluency on 500 µm Ø FN patterns in DMEM medium, 10 % FCS, allowed to attach 4 hours, washed with culture medium, then live imaged (phase contrast and fluorescence) at low magnification (10x, Biostation^{TM},

Nikon) every 10 min for 36 hours. The monolayer behavior was analyzed from the time cells occupy entirely the patterns by PIV (Particle Imaging Velocimetry) performed on phase contrast images, to obtain instantaneous velocity fields and correlation length in motion within the cellular disks (Strale et al., 2015).

Florescence image acquisition and Fluorescence Recovery after Photobleaching

Preparations were imaged either with a wide field fluorescent microscope (Olympus IX81) equipped of 60x oil immersion objective and a Coolsnap HQ ccd camera, or with a Leica Sp5-II confocal microscope with a 63 X oil immersion objective with a distance of .5 µm between each plane in the z-stacks. Fluorescence recoveries after photobleaching were performed at 37°C on GFP-α-catenin expressing cells, 24 hours post-transfection, using the Leica Sp5-II setup.

Protein recruitments at cell-cell contacts were determined on z-stack confocal images encompassing the apical cell domain of the monolayer (3 most apical stacks) analyzed the "surfaces" module of Imaris software, applying background subtraction, thresholding of junction area and removal objects outside junctions. Then the mean intensities of the different staining were measured in the volume of junctions.

Magnetic tweezers cytometry

Ecad-Fc-coated bead doublets attached to the surface of transfected cells were submitted to magnetic twisting using an in-house built magnetic tweezers. Bead doublets were used instead of individual beads to increase the applied torque and facilitate subsequent image analysis. Bead doublet rotation was captured while the rotation of the magnet was

simultaneously recorded. The fluctuation angle of the bead doublet relative to its original direction was calculated to obtain its response to magnet rotation, and the standard deviation of the fluctuation angle was extracted.

Life time of cell-cell contacts

The appearance and disappearance of individual cell-cell contacts were tracked over time on time-laps of RFP-Ftractin fluorescence movies. The *t* zero was set when two cells initiate a contact and the separation time, the time at which the two cells separated within the monolayer.

Statistical analysis and curve fitting and image processing

Statistical analysis and curves fitting were performed with GraphPad Prism 5.0 software. Image processing were done in Image J (or Matlab when indicated), then with Photoshop and Illustrator.

Acknowledgements:

This work was supported by grants from CNRS, Université Paris-Diderot (RMM,BL), NUS-SPC joined program (RMM), Fondation ARC (RMM), Human Frontier Science Program (HFSP) grant RPG0040/2012 (B.L., R.M.M.), Agence Nationale de la Recherche (ANR 2010 Blan1515). BL is supported by the European Research Council under the European Union's Seventh Framework Programme (FP7/2007–2013/ERC grant agreement no. 617233) and the Mechanobiology Institute. R.S. has been supported by a C'nano program Région Ile de France doctoral fellowship and FRM (FDT20140930851). The authors acknowledge the Institut du Fer à Moulin Cell Imaging Facility and the IJM Imagoseine Imaging Facility, member of the France BioImaging infrastructure supported by the French National Research Agency (ANR-10-INSB-04, « Investments of the future »). We thank the member of the Cell Adhesion and Mechanics group for discussions and constant support, as well as colleagues of the Institut Jacques Monod. MDCK αE-catenin knockdown cells were kindly provided by Dr. W. James Nelson (Stanford, US).

References

Bazellieres, E., V. Conte, A. Elosegui-Artola, X. Serra-Picamal, M. Bintanel-Morcillo, P. Roca-Cusachs, J.J. Munoz, M. Sales-Pardo, R. Guimera, and X. Trepat. (2015). Control of cell-cell forces and collective cell dynamics by the intercellular adhesome. *Nat Cell Biol*. 17:409-420.

Benjamin, J.M., A.V. Kwiatkowski, C. Yang, F. Korobova, S. Pokutta, T. Svitkina, W.I. Weis, and W.J. Nelson. (2010). AlphaE-catenin regulates actin dynamics independently of cadherin-mediated cell-cell adhesion. *J Cell Biol*. 189:339-352.

Chen, C.S., S. Hong, I. Indra, A.P. Sergeeva, R.B. Troyanovsky, L. Shapiro, B. Honig, and S.M. Troyanovsky. (2015). alpha-Catenin-mediated cadherin clustering couples cadherin and actin dynamics. *J Cell Biol*. 210:647-661.

Collins, C., and W.J. Nelson. (2015). Running with neighbors: coordinating cell migration and cell-cell adhesion. *Curr Opin Cell Biol*. 36:62-70.

Desai, R., R. Sarpal, N. Ishiyama, M. Pellikka, M. Ikura, and U. Tepass. (2013). Monomeric α-catenin links cadherin to the actin cytoskeleton. *Nature cell biology*. 15:261-273.

Doxzen, K., S.R. Vedula, M.C. Leong, H. Hirata, N.S. Gov, A.J. Kabla, B. Ladoux, and C.T. Lim. (2013). Guidance of collective cell migration by substrate geometry. *Integr Biol (Camb)*. 5:1026-1035.

Dufour, S., R.M. Mege, and J.P. Thiery. (2013). alpha-catenin, vinculin, and F-actin in strengthening E-cadherin cell-cell adhesions and mechanosensing. *Cell Adh Migr*. 7:345-350.

Guillot, C., and T. Lecuit. (2013). Mechanics of epithelial tissue homeostasis and morphogenesis. *Science*. 340:1185-1189.

Han, M.K., E. Hoijman, E. Noel, L. Garric, J. Bakkers, and J. de Rooij. (2016). alphaE-catenin-dependent mechanotransduction is essential for proper convergent extension in zebrafish. *Biol Open*. 5:1461-1472.

Hansen, S.D., A.V. Kwiatkowski, C.Y. Ouyang, H. Liu, S. Pokutta, S.C. Watkins, N. Volkmann, D. Hanein, W.I. Weis, R.D. Mullins, and W.J. Nelson. (2013). alphaE-catenin actin-binding domain alters actin filament conformation and regulates binding of nucleation and disassembly factors. *Mol Biol Cell*. 24:3710-3720.

Hoffman, B.D., and A.S. Yap. (2015). Towards a Dynamic Understanding of Cadherin-Based Mechanobiology. *Trends Cell Biol*. 25:803-814.

Huveneers, S., and J. de Rooij. (2013). Mechanosensitive systems at the cadherin-F-actin interface. *Journal of Cell Science*. 126(Pt 2) 403-413.

Jurado, J., J. de Navascues, and N. Gorfinkiel. (2016). alpha-Catenin stabilises Cadherin-Catenin complexes and modulates actomyosin dynamics to allow pulsatile apical contraction. *J Cell Sci*. 129:4496-4508.

Kim, T.J., S. Zheng, J. Sun, I. Muhamed, J. Wu, L. Lei, X. Kong, D.E. Leckband, and Y. Wang. (2015). Dynamic visualization of alpha-catenin reveals rapid, reversible conformation switching between tension states. *Curr Biol*. 25:218-224.

Ladoux, B., W.J. Nelson, J. Yan, and R.M. Mege. (2015). The mechanotransduction machinery at work at adherens junctions. *Integr Biol (Camb)*. 10 1109-1119.

le Duc, Q., Q. Shi, I. Blonk, A. Sonnenberg, N. Wang, D. Leckband, and J. de Rooij. (2010). Vinculin potentiates E-cadherin mechanosensing and is recruited to actin-

anchored sites within adherens junctions in a myosin II-dependent manner. *The Journal of cell biology*. 189:1107-1115.

Leckband, D., and A. Prakasam. (2006). Mechanism and dynamics of cadherin adhesion. *Annu Rev Biomed Eng*. 8:259-287.

Lien, W.H., O. Klezovitch, T.E. Fernandez, J. Delrow, and V. Vasioukhin. (2006). alphaE-catenin controls cerebral cortical size by regulating the hedgehog signaling pathway. *Science*. 311:1609-1612.

Maki, K., S.W. Han, Y. Hirano, S. Yonemura, T. Hakoshima, and T. Adachi. (2016). Mechano-adaptive sensory mechanism of alpha-catenin under tension. *Sci Rep*. 6:24878.

Mayor, R., and S. Etienne-Manneville. (2016). The front and rear of collective cell migration. *Nat Rev Mol Cell Biol*. 17:97-109.

Mege, R.M., and N. Ishiyama. (2017). Integration of Cadherin Adhesion and Cytoskeleton at Adherens Junctions. *Cold Spring Harb Perspect Biol*.

Peng, X., L.E. Cuff, C.D. Lawton, and K.A. DeMali. (2010). Vinculin regulates cell-surface E-cadherin expression by binding to beta-catenin. *J Cell Sci*. 123:567-577.

Peng, X., J.L. Maiers, D. Choudhury, S.W. Craig, and K.a. DeMali. (2012). α-Catenin uses a novel mechanism to activate vinculin. *The Journal of biological chemistry*. 287:7728-7737.

Ray, S., H.P. Foote, and T. Lechler. (2013). beta-Catenin protects the epidermis from mechanical stresses. *J Cell Biol*. 202:45-52.

Silvis, M.R., B.T. Kreger, W.H. Lien, O. Klezovitch, G.M. Rudakova, F.D. Camargo, D.M. Lantz, J.T. Seykora, and V. Vasioukhin. (2011). alpha-catenin is a

tumor suppressor that controls cell accumulation by regulating the localization and activity of the transcriptional coactivator Yap1. *Sci Signal*. 4:ra33.

Strale, P.O., L. Duchesne, G. Peyret, L. Montel, T. Nguyen, E. Png, R. Tampe, S. Troyanovsky, S. Henon, B. Ladoux, and R.M. Mege. (2015). The formation of ordered nanoclusters controls cadherin anchoring to actin and cell-cell contact fluidity. *J Cell Biol*. 210:333-346.

Takeichi, M. (2014). Dynamic contacts: rearranging adherens junctions to drive epithelial remodelling. *Nat Rev Mol Cell Biol*. 15:397-410.

Thomas, W.A., C. Boscher, Y.S. Chu, D. Cuvelier, C. Martinez-Rico, R. Seddiki, J. Heysch, B. Ladoux, J.P. Thiery, R.M. Mege, and S. Dufour. (2013). alpha-Catenin and vinculin cooperate to promote high E-cadherin-based adhesion strength. *J Biol Chem*. 288:4957-4969.

Torres, M., A. Stoykova, O. Huber, K. Chowdhury, P. Bonaldo, A. Mansouri, S. Butz, R. Kemler, and P. Gruss. (1997). An alpha-E-catenin gene trap mutation defines its function in preimplantation development. *Proc Natl Acad Sci U S A*. 94:901-906.

Vasioukhin, V., C. Bauer, L. Degenstein, B. Wise, and E. Fuchs. (2001). Hyperproliferation and defects in epithelial polarity upon conditional ablation of alpha-catenin in skin. *Cell*. 104:605-617.

Vedula, S.R., M.C. Leong, T.L. Lai, P. Hersen, A.J. Kabla, C.T. Lim, and B. Ladoux. (2012). Emerging modes of collective cell migration induced by geometrical constraints. *Proc Natl Acad Sci U S A*. 109:12974-12979.

Vedula, S.R., A. Ravasio, E. Anon, T. Chen, G. Peyret, M. Ashraf, and B. Ladoux. (2014). Microfabricated environments to study collective cell behaviors. *Methods Cell Biol*. 120:235-252.

Vermeulen, S.J., E.A. Bruyneel, M.E. Bracke, G.K. De Bruyne, K.M. Vennekens, K.L. Vleminckx, G.J. Berx, F.M. van Roy, and M.M. Mareel. (1995). Transition from the noninvasive to the invasive phenotype and loss of alpha-catenin in human colon cancer cells. *Cancer Res*. 55:4722-4728.

Yao, M., W. Qiu, R. Liu, A.K. Efremov, P. Cong, R. Seddiki, M. Payre, C.T. Lim, B. Ladoux, R.M. Mege, and J. Yan. (2014). Force-dependent conformational switch of alpha-catenin controls vinculin binding. *Nat Commun*. 5:4525.

Yonemura, S., Y. Wada, T. Watanabe, A. Nagafuchi, and M. Shibata. (2010). alpha-Catenin as a tension transducer that induces adherens junction development. *Nature cell biology*. 12:533-542.

Figure Legends

Figure 1: Substrate stiffness-dependent recruitment of α-catenin, vinculin and F-actin at cell-cell contacts

(A) MDCK cells were cultured for 24 hours on PPA gels of the indicated stiffness (4.5 , 9 or 35 kPa), on which 100 µm diameter disks of FN had been patterned. Preparations were then fixed and immunostained for α-catenin, α18 epitope, vinculin, and F-actin, and then imaged by confocal microscopy (panels show 0.5 µ thick z-projections taken at the level of the apical complexes). Scale bar: 50 µm. **(B)** The histograms represent the mean fluorescence intensity measured for αE-catenin, α18 epitope, vinculin and F-actin stainings at cell-cell contacts as indicated in Materials and Methods (mean ± SEM, n = 640 to 1260 junctions total out of 3 independent experiments, *** $p< 0.0001$. **(C)** Western blot analysis of α-catenin and vinculin from protein extracts of cells grown for 24 hours on FN coated PAA gels of 4.5, 9 and 35 kPa rigidity, respectively. α-tubulin was used as a loading control.

Figure 2: E-cadherin-dependent cell-cell contacts form independently of α-catenin/vinculin interactions

(A) Schematics of GFP-tagged wt (α-cat-WT-GFP), L344P (α-cat-L334P-GFP) and Δmod (α-cat-Δmod-GFP) αE-catenin constructs. **(B)** Confocal analysis of vinculin and F-actin distribution in αE-catenin KD MDCK cells expressing α-cat-WT-GFP, α-cat-L334P-GFP and α-cat-Δmod-GFP grown on glass surfaces (1 µm thick subapical confocal sections). The expression of mutant proteins restores apparently normal cell-cell

contacts, as does the expression of wt α-catenin. Scale bar: 5 μm. **(C)** FRAP experiments were performed on cell-cell contacts of α-cat-WT-GFP (green), α-cat-L334P-GFP (blue) or α-cat-Δmod-GFP (red) expressing cells grown on glass substrates. Mean intensity recoveries over time (± SEM) fitted with a one-term exponential equation (n= 50 regions of interest out of 3 independent experiments for each condition). **(D)** Mobile fractions extracted from the fits of individual recovery curves (mean values ± SD and 95th percentile). *** $p < 0.0001$, ns: non-significant.

Figure 3: Binding of α-catenin to vinculin is required for its tension-dependent stabilization at cell-cell contacts

(A, B) MDCK α-catenin-KD cells expressing GFP-tagged wt α-catenin (green), α-cat-L334P (blue) or α-cat-Δmod (red) were cultured for 24 hours on 4.5 (light colors) or 35 kPa (dark colors) PPA gels before FRAP experiments were performed. Graphs represent mean GFP fluorescence recovery over time (± SEM, n= 50 out of 3 independent experiments for each condition) fitted with a one-term exponential equation. **(C)** Mobile fraction values (mean values ± SD and 95th percentile) extracted from the fits of individual recovery curves considered in panels **A** and **B**. ** $p < 0.001$, ns: non-significant. Notice the non-significant differences in mobile fraction values observed for the mutant proteins on soft and stiff substrates, contrasting with the significant decrease in mobile fraction observed for the wt protein as a function of increasing substrate compliance. **(D)** Magnetocytometry applied on Ecad-Fc coated bead doublets bound to the surface of MDCK cells expressing GFP-tagged α-cat-wt, α-cat-L334P and α-cat-Δmod mutants. The histogram reports the mean values of the standard deviation of the

bead fluctuation angles. The mean bead deviation angle was close to 0 degree for α-cat-Δmod cells expressing**,** indicating a very stiff link of cadherins to the cortical actin. At the opposite, this value was close to 30 degrees for beads bound on α-cat-L334P expressing cells, indicating a loose mechanical association of the beads to the cell cortex.

Figure 4: Vinculin/α-catenin association controls collective cell behavior and cell-cell contact lifetime

(A) MDCK cells silenced for α-catenin (α-cat KD), as well as cells expressing GFP-tagged α-cat-L334P, α-cat-Δmod or GFP-tagged wt α-catenin (α-cat-wt), were seeded on 500 μm Ø FN patterns and phase contrast imaged for 24-36 hours (panels provide still images, see supplementary videos 1 to 4). The collective behavior of cell monolayers was analyzed by PIV over 6 hours providing heat maps of instantaneous local velocities **(B)**. Mean velocities **(C)** and correlation lengths **(D)** characteristic of each cell type were then extracted from these instantaneous velocity map (mean values ± SD) out of 3 independent experiments, n = 360 frames analyzed per condition, derived from 10 patterns per condition coming from 3 independent experiments. *** $p<0.0001$, ** $p<0.001$, * $p<0.01$, ns: non-significant. **(E)** Mean lifetime of individual cell-cell contacts measured for each cell type (wicker plot: mean ± SD and 95th percentile, n = 30 cell doublets for α-cat KD and α-cat-wt, and n= 51 for α-cat-L334P, α-cat-Δmod, respectively, out of ≥ 4 patterns derived from ≥ 2 independent experiments for each condition, *** $p<0.0001$, ** $p<0.001$).

Figure 1: Seddiki

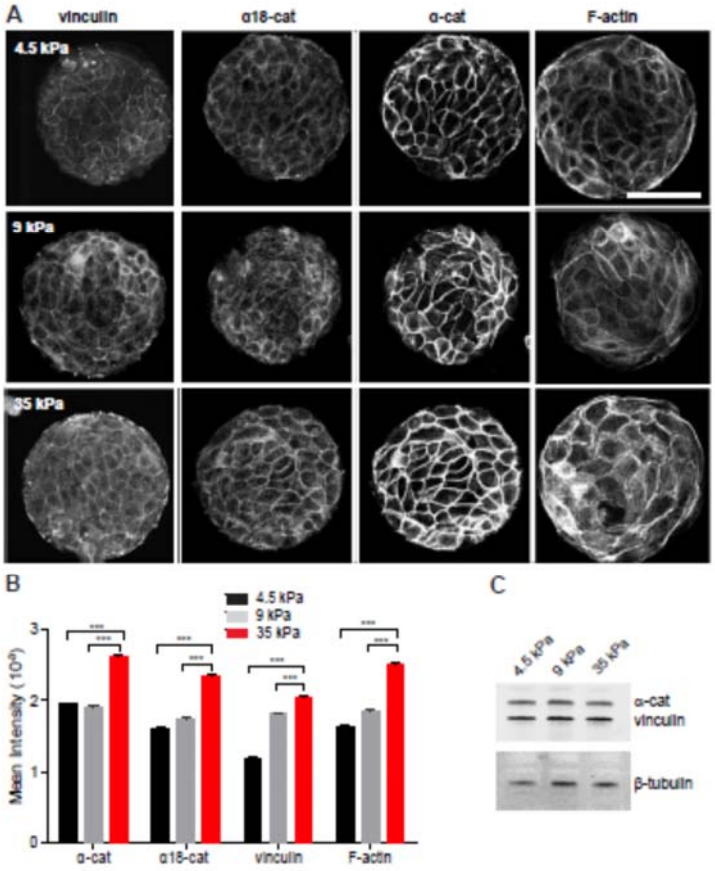

Figure 2: Seddiki

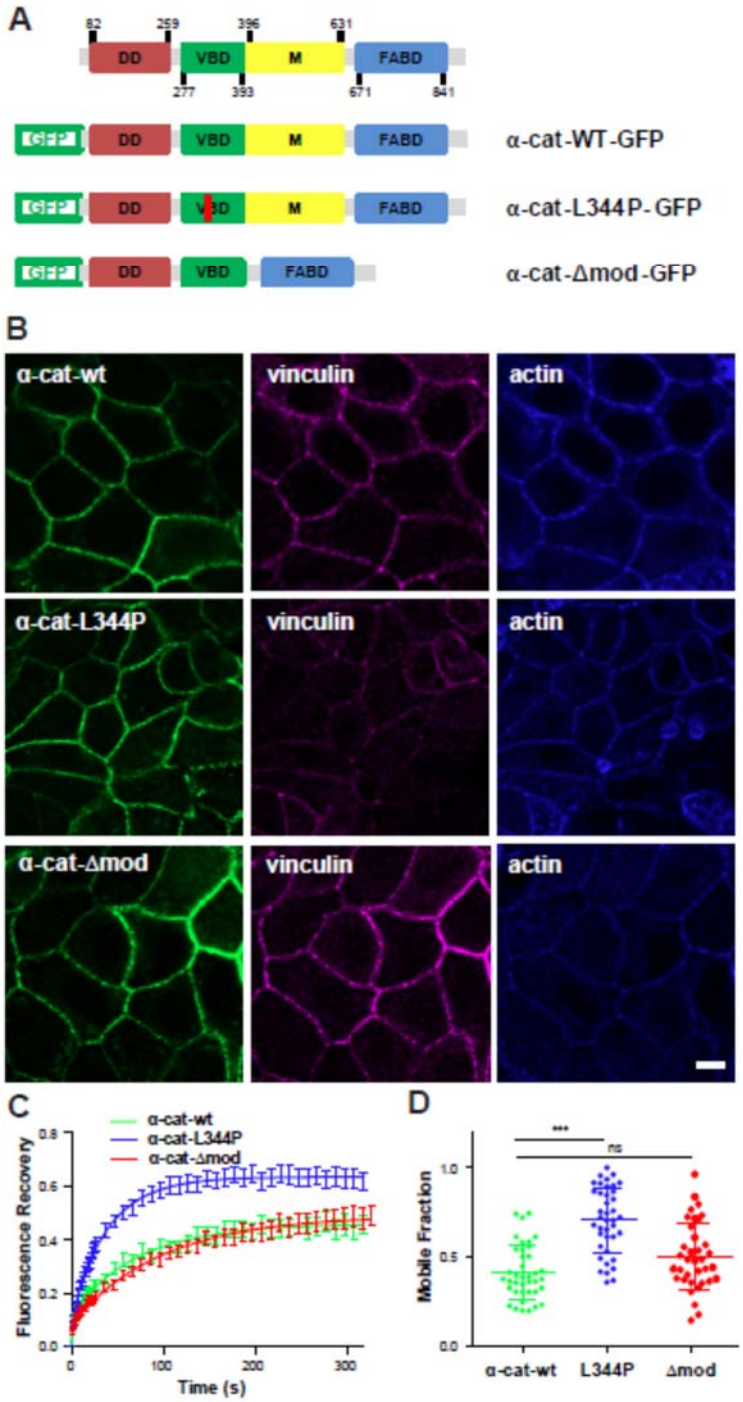

Figure 3: Seddiki

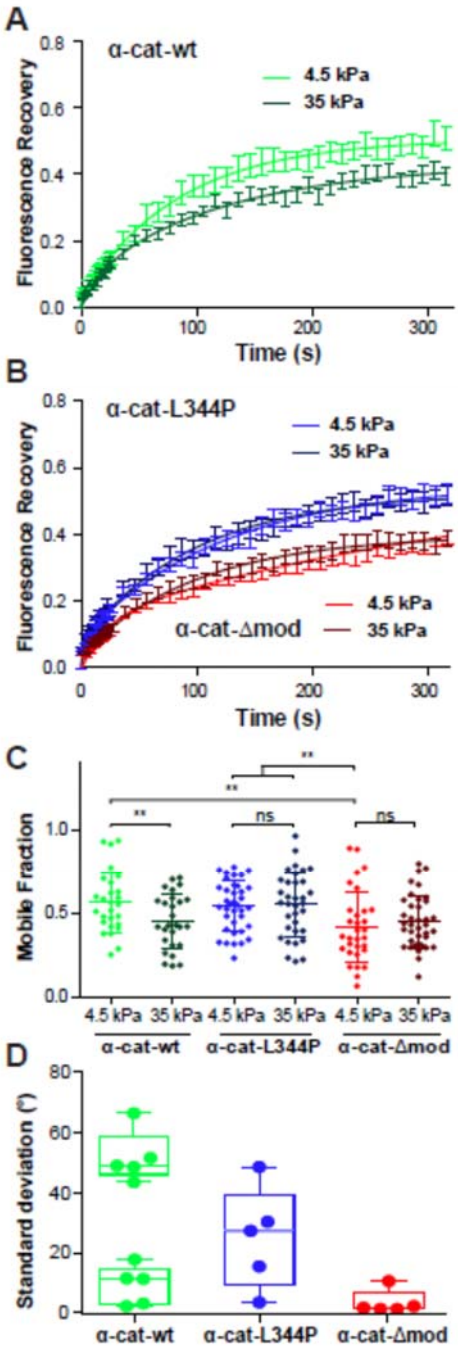

Figure 4: Seddiki